Probabilistic demand and supply resilience model for electric power supply system under seismic hazard

Conference Paper

Author(s):
Sun, Li; Didier, Max; Delé, Eric; Stojadinovic, Bozidar

Publication date:
2015-07

Permanent link:
https://doi.org/10.3929/ethz-b-000559710

Originally published in:
https://doi.org/10.14288/1.0076148

Probabilistic Demand and Supply Resilience Model for Electric Power Supply System under Seismic Hazard

Li Sun
Ph.D. Candidate, Institute of Structural Engineering, Swiss Federal Institute of Technology (ETH) Zurich, Zurich, Switzerland

Max Didier
Ph.D. Candidate, Institute of Structural Engineering, Swiss Federal Institute of Technology (ETH) Zurich, Zurich, Switzerland

Eric Delé
Master Student, Institute of Structural Engineering, Swiss Federal Institute of Technology (ETH) Zurich, Zurich, Switzerland

Bozidar Stojadinovic
Professor, Institute of Structural Engineering, Swiss Federal Institute of Technology (ETH) Zurich, Zurich, Switzerland

ABSTRACT: A compositional framework for the probabilistic assessment of the seismic resilience of an electric power supply system and a community it serves is proposed and illustrated in this paper. This framework is based computing the electric power supplied by the system and the electric power demand generated by the community through the earthquake damage absorption and recovery phases. Losses occurring when the demand exceeds the supply are a direct measure of the lack of EPSS resilience. During the damage absorption phase, the loss of system supply and the community demand is computed using component vulnerability functions. An inverse computation is done during the recovery phase using component recovery functions, defined as conditional probability that a component function will be fully restored after a certain recovery time period given its damage level. The integration of the component vulnerability and recovery functions for the electric power supply system considers the topology of the system, its function, and the correlations among its components. Similarly, integration of the community component vulnerability and recovery functions can account for the social and economical interactions in the community. A case study using a portion of the IEEE 118 Bus Test Case is used to illustrate the framework, develop a set of vulnerability and recovery functions, and compute direct and derived electrical power supply system seismic resilience measures.

Seismic resilience of the Electric Power Supply System (EPSS) is critical to the seismic resilience of a community (Franchin and Cavalieri 2014; Mieler et al. 2014). The topology of a modern EPSS is complex and its components are diverse. Similarly, the components of a community, viewed only from the standpoint of electrical power demand, are diverse and interconnected. Generally, an EPSS consists of the power generation, power transmission, and power distribution sub-systems, each of which is comprised of numerous interconnected components. Under normal operating conditions the state of an EPSS, measured through the difference between the electricity supplied by the system and the electricity demanded by the customers in the communities it serves, is stable. Conversely, the state of an EPSS may be very dynamic in the aftermath of an earthquake, reflecting the sudden changes in both supply and demand (Liu et al. 2012; Hollnagel and Fujita 2013). This renders the post-earthquake relationship between the electric power supply and demand for an EPSS stochastic and intertwined.

A compositional framework for the probabilistic assessment of the seismic resilience of an EPSS is proposed in this paper. Instead of quantifying the evolution of the seismic response of EPSS in the aftermath of an earthquake using a single parameter Q to measure system functionality (Bruneau et al. 2003), the proposed framework tracks the post-earthquake evolution of the supply provided by the EPSS and the demand generated by the customers in the community (Figure 1).

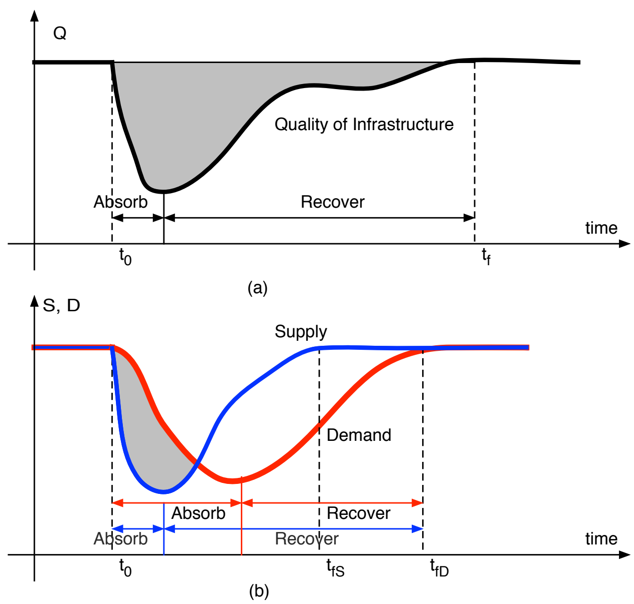

Figure 1: Measures of seismic resilience: (a) single parameter (Bruneau et al., 2003); (b) proposed supply/demand comparison.

The difference between the electricity supply, representing the ability of the EPSS to function, and demand, representing the ability of the community to function, is a direct measure of EPSS resilience. The evolution of the supply/demand difference is tracked through time after the occurrence of the earthquake, divided into the Absorb and the Recovery phases (Ouyang et al. 2012). Clearly, failure of the EPSS occurs when it supplies less electricity than the community needs: thus, the EPSS may provide sufficient power, even if it functions below its capacity, compared to the diminished ability of the damaged community to use the power.

Resilience of an EPSS is computed using a compositional approach. During the (relatively short) Absorb phase, the loss of EPSS supply and the community demand is computed using component vulnerability functions (probability of loss of function, directly related to incurred damage, conditioned on the earthquake intensity measure) and integrating at the EPSS and community levels. An inverse computation is done during the (relatively long) Recovery phase. To facilitate the compositional approach, component recovery functions (probability that a component function will be fully restored after a certain recovery time period, conditioned on the level of component damage) are introduced. At a given time in the Recovery phase, the EPSS supply and community demand are computed by integrating at the recovery function within the two systems. The integration of the component vulnerability and recovery functions within a system considers the topology of the system and the correlations among its components. The, presumably, weaker correlations between the components of the two systems, and system-level interaction are neglected.

The separation of the supply provided by the infrastructure system and the demand generated in the community enables formulation and quantification of indirect measures of resilience. Such measures, e.g. time evolution of the number of people without power after an earthquake, are socially and economically meaningful and can be used to inform infrastructure investment, urban planning and public policy decisions.

1. CASE STUDY

The proposed compositional framework for seismic resilience assessment of infrastructure systems is illustrated using an simplified earthquake scenario affecting the example EPSS network and the community it serves (Figure 2).

A portion of the IEEE 118 Bus Test Case is used to represent the EPSS network. This is a realistic network that "represents a portion of the American Electric Power System (in the

Midwestern US) as of December, 1962" (Christie 1993). For simplicity, only 34 nodes of the original 118-node network are used in this case study. The network nodes correspond to high, medium and low voltage electric substations. High voltage nodes (red) are the electrical power supply nodes (generation stations, transmission substations), whereas medium and low voltage nodes (blue) are the transmission and distribution substation nodes.

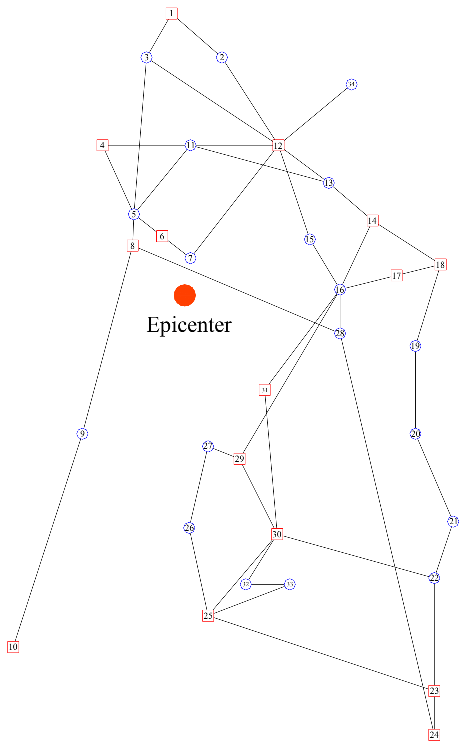

Figure 2: Topology of the case study EPSS and the community it serves.

A generation substation (Figure 3) consists of two main 220 kV bus bars (81 and 82) and one reserve 220 kV bus bar (83) on each side that are connected with a circuit breaker. Generators (61 and 62) are attached to each main bar. The reserve bus bar can replace either the input or the output bus bar using an appropriate configuration of the circuit breakers (11 through 17).

A distribution substation (Figure 4) also consists of two main bus bars (81 and 82) and one reserved bus bar (83). Transformers (61, 62 and 63) reduce the 220 kV input voltage to the 35 kV output voltage. A distribution substation has two different outputs: one for high-voltage current flow, and one for the transformed low-voltage current flow. The circuit breakers (11 through 21) facilitate the operation of the substation and the engagement of the reserve bus bar when necessary.

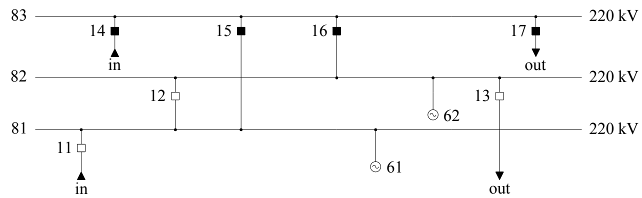

Figure 3: A generation substation.

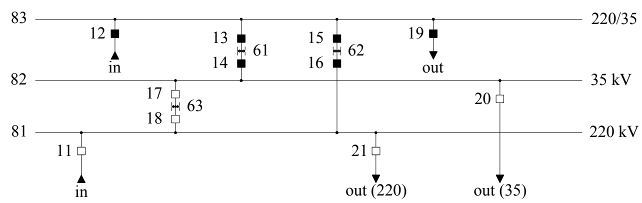

Figure 4: A distribution substation.

The case study EPSS (Figure 2) has 15 generation substations and 19 distribution substations. The gross amount of electric power it supplies under normal operation conditions can be calculated by adding the power generation capacity of each generation substations.

The community supplied by the EPSS is significantly more difficult to model. To reduce the complexity, only three types of structures are included in the community model: residential, industrial, and critical facility structures. They are further subdivided into categories (Table 1).

Table 1: Community structure types.

Residential	RC apartment building
	Masonry apartment building
	Masonry single-family house
Industrial	Heavy industry
	Light industry
	Office building
Critical Facility	Hospital
	School

A total of 36 residential, industrial and critical facility components were assumed to be at sites in close proximity to one of the electric power distribution substations. The specific numbers of different types of structures that were assigned at a site was determined using average amounts of residential, industrial and critical facility power demand obtained from different data sources (Déle and Didier 2014) and the power supply provided by the nearby substation.

The simplified seismic hazard environment was modeled by locating the hypocenter of an earthquake close to the geographic center of the case study grid (Figure 2). The intensity of shaking at each EPSS or community component site, measured using peak ground motion displacement, velocity and acceleration values, was computed using the ground motion attenuation relations proposed in (Campbell and Bozorgnia 2008). The magnitude of the earthquake was associated with the hazard using a Gutenberg-Richter law with a=4.4 and b=1 (Kramer 1996), modified using a magnitude 4.5 lower and magnitude 7.5 upper bound (smaller earthquakes were disregarded, larger earthquakes were counted as magnitude 7.5 events).

A case study simulation started by assuming an earthquake of magnitude M occurred at the epicenter. Intensities of the ground motion at the EPSS and community components sites were computed using attenuation functions.

1.1. Absorption phase

In the immediate aftermath of an earthquake the EPSS and the community it supplies undergo a relatively short period of damage absorption. The induced damage of the components of the EPSS and the community structures was classified into three damage states:

- DS1: no damage;
- DS2: slight/moderate damage; and
- DS3: extensive damage/collapse.

This classification was accomplished using a variety of fragility functions found in literature.

For the EPSS components, Shinozuka et al. (2007) and the Syner-G project (Cavalieri et al. 2014) developed fragility functions for transformers, circuit breakers and bus bars based on empirical data from the 1994 Northridge earthquake. Only DS1 and DS3 damage states are considered for these components. The fragility functions for the small (less than 200MW) and large (more than 200MW) power generation were found in HAZUS (FEMA 2003). Damage to transmission lines was not considered.

Different fragility functions were chosen for different components of the community built environment. The fragility functions developed by Rossetto and Elnashai (2003), typical for European residential construction, were used for the reinforced concrete buildings. Similarly, fragility functions developed by Karantoni et al. (2011) for typical 4- and 2-story European masonry buildings were used for the masonry apartment and single-family structures. Jeong and Elnashai (2007) developed worldwide-applicable fragility functions for 12-storey reinforced concrete buildings that were adopted for the office buildings. Senel and Kayhan (2009) developed PGV-based fragility functions for pre-cast industrial buildings in Turkey whose parameters were adjusted to model damage in heavy and light industry structures. The fragility functions for mid-rise RC buildings developed by Kwon and Elnashai (2006) were used to model school buildings. Finally, it was assumed that the hospital buildings would not develop significant structural damage, but would develop non-structural damage affecting the medical equipment that consumes significant amounts or electricity or the facilities (room ceilings, walls, doors, corridors, elevators, storage, water supply) where medical services are delivered. Such non-structural damage would result in a significant reduction of electrical power demand. The fragility data developed in the Syner-G project (Lupoi et al. 2014) was used to determine the power loss within the hospitals after an earthquake.

The vulnerability of the EPSS was quantified by evaluating the drop in the electricity supplied by the EPSS to the components of the community caused by earthquake damage to EPSS components. The supply of electricity depends on the ability to generate power as well as the available transition paths. The damage states of the generators were evaluated first to determine if they are fully or partially operational. The states of substation components were evaluated, followed by an analysis of the entire substation to determine the available electricity paths and the remaining grid connectivity. Then a flow balance analysis was conducted to determine which demand nodes are supplied with how much power (Delé and Didier 2014).

Similarly, the vulnerability of the community was quantified by evaluating a drop in the electricity demand. This drop was computed for each community component by correlating its damage state to the amount of electricity it can consume after an earthquake. If a structure is in damage state DS1 (no damage), it was assumed that its power demand would remain at the pre-earthquake level. Conversely, if the structure is in damage state DS3 (extensive damage) it would consume no power.

Determining the power demand form structures in damage state DS2 is challenging. In this case study, it was assumed that the power demand is at most 90% of the pre-earthquake demand, and that it further depends on the level of damage to structures in the community. This level of damage was assessed by evaluating portion of buildings in damage state DS3 relative to the total number of building in the considered category. The number of buildings in this damage state was assumed to be quite uncertain right after the earthquake, but becoming more accurate as the building inspection and tagging proceeds. To model this, the number of buildings in damage state DS3 was modeled using a lognormal probability distribution function with a mean taken as the value calculated from the fragility functions and the standard deviation computed as a function of the number of days t after the earthquake as follows:

$$\sigma_{DS3} = \begin{cases} 1 - 0.2t & t \leq 5 \\ 0 & t > 5 \end{cases} \quad (1)$$

The power demand from residential buildings in DS2 was assumed to depend on the level of damage in the neighborhood (labeled *local*), taken as the residential location supplied by the same EPSS distribution node in this case study. Conversely, the power demand generated by the industrial buildings was assumed to strongly depend on the state of the entire community, including the state of other infrastructure systems and the economic and social impact of the earthquake. A simplistic model based on the ratio of number of industrial buildings in DS3 versus the total number of industrial buildings in the community was used in this case study. Finally, it was assumed that critical facilities in DS2 would continue to draw power at the pre-earthquake level. This was justified by assuming that hospitals would continue to work at full capacity and that schools would serve as shelters. The electric power demand vulnerability model is shown in Table 2.

Table 2: Correlation between electric power demand and damage states of structures.

Structure Category	DS1	DS2	DS3
Residential	100%	$\left(1 - \frac{\mathrm{DS3_{local}}}{\mathrm{DS_{1+2+3,local}}}\right) * 90\%$	0%
Industrial	100%	$\left(1 - 2\frac{\mathrm{DS3_{total}}}{\mathrm{DS_{1+2+3,total}}}\right) * 90\%$	0%
Critical	100%	100%	0%

1.2. Recovery phase

After absorbing the incurred earthquake damage, the EPSS and the community it supplies enter a relatively long recovery period. Component recovery functions expressing the probability that a component electric power function will be fully restored after a certain recovery time period, conditioned on the level of component damage, were developed to model the recovery process. In this sense, recovery functions are orthogonal to the vulnerability functions. Therefore, recovery functions were defined using a lognormal probability distribution. The parameters of these distributions were assumed for different components of the EPSS and the community based on limited data on post-earthquake recovery rates observed in recent earthquakes in China and Europe (Delé and Didier 2014). These parameters were also varied to evaluate the sensitivity of the simulation outcomes.

2. CASE STUDY RESULTS

A simulation of EPSS and community earthquake damage absorption and recovery was repeated 2000 times for each earthquake moment magnitude. The probability distributions representing the vulnerability and recovery functions were sampled using the Monte Carlo method.

2.1. Direct measure of seismic resilience

The mean results for an M=7.5 earthquake scenario are plotted in Figure 5. Before the earthquake, the EPSS supplied 900 MW satisfy the 733 MW of community demand with some redundancy. Once the earthquake damage was absorbed, the total community electric power demand dropped to about 650 MW, but the total power generated dropped to 600 MW and the total power delivered dropped to 540 MW. The generation capability recovered above the demand level within 3 days, but the ability to deliver power reached the community demand level only after 10 days. This point in time marks the end of the losses due to lack of resilience of the EPSS. A direct measure of EPSS resilience is the area between the community electrical power demand curve (blue) and the EPSS power delivery curve (red). It expresses the lack of electrical power in MW-days.

The difference between the total generated and delivered power reflects the different rates of generation and distribution facility recovery assumed in this case study. Subsequently, the EPSS was able to deliver power as the damaged community was recovering, reflecting the assumption that the rates of structural damage repair are slower than the repair rates for the EPSS facilities.

In fact, the rates of community recovery are so slow that, in this case study, it took approximately 2000 days (roughly 6 years) for its power consumption to return to the pre-earthquake level. Note that the model assumes that the community long-term social and economic structure remains unaffected by the earthquake. If, however, many people and/or industrial facilities move out of the community, it may never recovery its electric power demand. Conversely, new investments in the recovery and rebuilding of the earthquake-stricken region may increase the economic activity leading to an increase in the electric power demand.

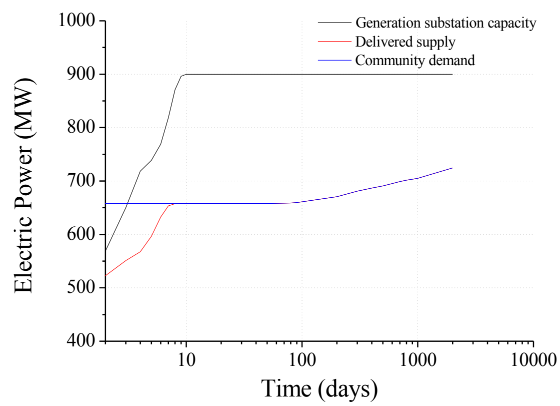

Figure 5: Electrical power supply/demand resilience evaluation for a magnitude 7.5 earthquake scenario.

2.2. Social and economic measure of seismic resilience

Even though the EPSS and the community models used in this case study are simplistic, the compositional approach to evaluating resilience enables conceptualization, formulation and quantitative evaluation of resilience metrics that have social and economic meaning.

One such derived resilience metric is the evolution of percentage of people (inhabitants in residential buildings) without electric power. In Figure 6, the mean percentage of people without power is plotted as a function of days after the M=7.5 scenario earthquake. Approximately 35% of the community population had no electric power 24 hours after the earthquake. Then the percentage of people affected by the blackout decreased slowly at the beginning of the recovery process. More than 25% of the population would be without electricity on the fourth day after the earthquake, while it would take 10 days to provide power to everyone who can use it. This recovery rate matches the observation made after recent major earthquakes.

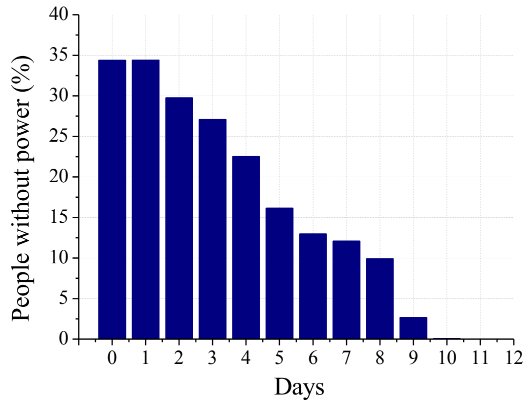

Figure 6: Percentage of the population affected by power outage.

The percentage of community population without power 24 hours after the earthquake is another useful derived EPSS resilience metric. This metric was computed for scenario earthquakes with moment magnitudes ranging from 4.5 to 7.5 and plotted in Figure 7.

There is a roughly linear relation between earthquake moment magnitude and the percentage of population without power 24 hours after the earthquake for earthquake moment magnitudes between 5 and 7. The curve flattens on both ends of the graphs. For low-magnitude earthquakes, the substations rarely fail indicating that the EPSS will be resilient and will supply the required power. On the other hand, most of the EPSS components in the vicinity of the epicenter will fail during high-magnitude earthquakes leading to saturation in the number of people without power. Thus, the losses due to lack of resilience of the EPSS could be capped. In turn, this data can be used to determine which portions of the EPSS should be hardened to increase its overall resilience and to evaluate different options. For example, it may be more economical to increase the grid connectivity rather than to strengthen individual distribution substations to enable more ways to deliver power to the community facilities in a region near the likely epicenter.

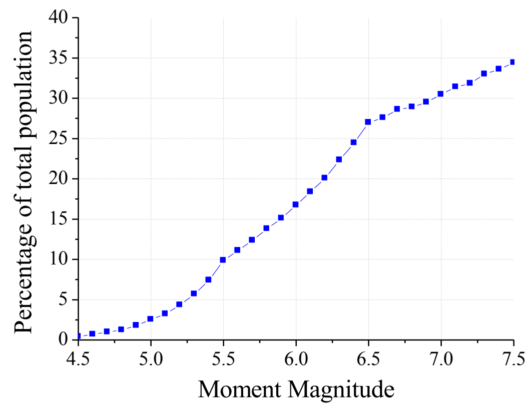

Figure 7: Percentage of total population out of power after one day versus the earthquake moment magnitude.

3. CONCLUSIONS

A compositional framework for the probabilistic assessment of seismic resilience of an infrastructure system was proposed and illustrated in this paper. The framework is based on a direct comparison of the supply provided by the infrastructure system and the demand generated by the community. The evolution of the supply/demand difference is tracked through time after the occurrence of the earthquake. Losses are incurred when the demand exceeds the supply, indicating a lack of infrastructure system resilience.

Resilience of the infrastructure system is computed using a compositional approach. During the damage absorption phase, the loss of system supply and the community demand is computed using component vulnerability functions. An inverse computation is done during the recovery phase using component recovery functions, defined as conditional probability that a component function will be fully restored after a certain recovery time period given its damage level. The integration of the component vulnerability and recovery functions for the infrastructure system considers the topology of the system, its function, and the correlations among its components. Similarly, integration of the community component vulnerability and recovery functions can account for the social and economical interactions in the community.

The granularity of the proposed framework enables formulation and quantification of infrastructure system resilience measures that have clear social and economic meaning. Such measures can be used as a basis for formulating community and infrastructure system risk governance policies and measures.

4. EFERENCES

Bruneau, M., Chang, S. E., and Eguchi, R. T. et al. (2003). "A Framework to Quantitatively Assess and Enhance the Seismic Resilience of Communities" *Earthquake Spectra*, 19(4), 733-752.

Campbell, K.W., Bozorgnia, Y. (2008). "NGA Ground Motion Model for the Geometric Mean Horizontal Component of PGA, PGV, PGD and 5% Damped Linear Elastic Response Spectra for Periods Ranging from 0.01 to 10 s" *Earthquake Spectra*, 24(1), 139-171.

Cavalieri, F., Franchin, P., and Pinto, P.E. (2014). "Fragility Functions of Electric Power Stations", in K.Pitilakis et al. (eds.) *SYNER-G: Typology Definition and Fragility Functions for Physical Elements at Seismic Risk, Geotechnical, Geological and Earthquake Engineering 27*, Springer Science+Business Media Dordrecht.

Christie, R.D. (1993). "Power Systems Test Case Archive" *http://www.ee.washington.edu/research/pstca/pf118/pg_tca118bus.htm*.

Delé, E., and Didier, M. (2014). "Time-Varying Seismic Resilience of Electric Supply Systems" *Master Thesis*, ETH Zurich.

Franchin, P., and Cavalieri, F. (2014). "Probabilistic Assessment of Civil Infrastructure Resilience to Earthquakes" *Computer-Aided Civil and Infrastructure Engineering*, 00, 1-18.

FEMA. (2003). "HAZUS-MH Technical Manual".

Hollnagel, E., and Fujita, Y. (2013). "The Fukushima Disaster-Systemic Failures as the Lack of Resilience" *Nuclear Engineering and Technology*, 45(1), 13-20.

Jeong, S.H., and Elnashai, A.S. (2007). "Probabilistic fragility analysis parameterized by fundamental response quantities" *Engineering Structures*, 29(8), 1238-1251.

Karantoni, T., Lyrantzaki, F., Tsionis, G., and Fardis, M.N. (2011). "Analytical Fragility Functions for Masonry Buildings and Building Aggregates-UPAT methodology" Internal Report, *Syner-G Project 2009/2012.*

Kramer, S.L. (1996). *Geotechnical Earthquake Engineering*, Prentice Hall.

Kwon, O.S., and Elnashai, A. (2006). "The effect of material and ground motion uncertainty on the seismic vulnerability curves of RC structures" *Engineering Structures*, 28(2), 289-303.

Liu, R., Zhang, M., and Wu, Y. (2012). "Vulnerability Study of Electric Power Grid in Different Intensity Area in Wenchuan Earthquake" *Proceedings of the 15th World Conference on Earthquake Engineering, Portugal*, September 24-28.

Lupoi, A., Cavalieri, F., and Franchin, P. (2014). "Component Fragilities and System Performance of Health Care Facilities", in K.Pitilakis et al. (eds.) *SYNER-G: Typology Definition and Fragility Functions for Physical Elements at Seismic Risk, Geotechnical, Geological and Earthquake Engineering 27*, Springer Science+Business Media Dordrecht.

Mieler, M., Stojadinovic, B., Budnitz, R., Comerio, M., and Mahin, S. (2014). "A Framework for Linking Community-Resilience Goals to Specific Performance Targets for the Built Environment" *Earthquake Spectra*, June 5, published online.

Ouyang, M., Duenas-Osorio, L., and Min, X. (2012). "A Three-Stage Resilience Analysis Framework for Urban Infrastructure Systems" *Structural Safety*, 36-37, 23-31.

Rossetto, T., and Elnashai, A. (2003). "Derivation of vulnerability functions for European-type RC structures based on observational data" *Engineering Structures*, 25(10), 1241-1263.

Senel, S.M., and Kayhan, A.H. (2009). "Fragility based damage assessment in existing precast industrial buildings: A case study for Turkey" *Structural Engineering and Mechanics*, 34(1), 39-60.

Shinozuka, M., Dong, X., Chen, T.C., and Jin, X. (2007). "Seismic performance of electric transmission network under component failures" *Earthquake Engineering and Structural Dynamics*, 36, 227-244.